Crystal-field effects competing with spin-orbit interactions in NaCeO$_2$

P. Bhattacharyya, U. K. Rößler, and L. Hozoi

Institute for Theoretical Solid State Physics, Leibniz IFW Dresden, Helmholtzstrasse 20, 01069 Dresden, Germany

Ce compounds feature a remarkable diversity of electronic properties, which motivated extensive investigations over the last decades. Inelastic neutron scattering represents an important tool for understanding their underlying electronic structures but in certain cases a straightforward interpretation of the measured spectra is hampered by the presence of strong vibronic couplings. The latter may give rise to extra spectral features, which complicates the mapping of experimental data onto standard multiplet diagrams. To benchmark the performance of embedded-cluster quantum chemical computational schemes for the case of $4f$ systems, we here address the Ce $4f^1$ multiplet structure of NaCeO$_2$, an antiferromagnet with D_{2d} magnetic-site symmetry for which neutron scattering measurements indicate only weak vibronic effects. Very good agreement with the experimental results is found in the computations, which validates our computational approach and confirms NaCeO$_2$ as a $4f$ magnet in the intermediate coupling regime with equally strong $4f$-shell spin-orbit and crystal-field interactions.

I. INTRODUCTION

Spin-orbit interactions have received enormous attention in recent years. New insights and new ideas have led to new physical models, new concepts, and new research paths, as for example the Kitaev honeycomb model [1,2] and related extensive investigations. A very interesting aspect is the role of crystalline fields in realizing a particular type of magnetic ground state. For octahedral ligand coordination of d- or f-metal magnetic centers, not only the octahedral crystal-field splittings are relevant but also additional splittings related to lower-symmetry fields—tetragonal, trigonal, etc. The latter may originate from distortions of the ligand cages away from a regular, cubic octahedron and/or peculiarities of the crystalline lattice, e.g., from having a layered structure. The precise nature and strength of the underlying ligand/crystal fields are relevant to properties and parameters such as magnetic moments, single-ion anisotropies, and intersite exchange couplings. Spin-orbit interactions and crystal-field splittings meet sometimes on the same energy scale, in both d- [3–5] and f-electron systems [6–10]. This may give rise to, e.g., unexpected magnetic ground states [5]. It may also hamper a straightforward interpretation of experimental data [6] and may pose problems to computational modeling [11]. The Ce^{3+} oxide compounds are in this context representative, with spin-orbit couplings (SOCs) and crystal-field splittings of similar magnitude [6–9]. The $4f$-shell multiplet structure is relatively simple in these systems: For a Ce^{3+} $4f^1$ ion in symmetry lower than O_h, seven Kramers doublets are expected. The lowest three and upper four are degenerate in the case of a free ion, defining $J = 5/2$ and $J = 7/2$ free-ion terms. Interestingly, in delafossite [8,12] and pyrochlore [13,14] structures with D_{3d} Ce-site symmetry, one extra excitation is observed experimentally in the lower-energy range (i.e., within the $J = 5/2$-like energy window), likely arising from

strong vibronic couplings. For benchmark *ab initio* multiplet calculations in the intermediate coupling regime with equally strong $4f$-shell spin-orbit and crystal-field interactions, we here choose NaCeO$_2$ as a test case. It features D_{2d} Ce-site symmetry, and complications as seen in the D_{3d} setting [8,12–15] do not arise in this geometry [9]. Our study adds useful reference data to investigations addressing the electronic structure and the physical properties of Ce oxide compounds, providing a solid basis for extensions towards the computation of total energy landscapes and vibronic excitations.

II. COMPUTATIONAL DETAILS

Tetragonally distorted, edge- and corner-sharing CeO$_6$ octahedra form a bipartite diamond magnetic lattice in NaCeO$_2$, as depicted in Fig. 1(a). To understand the specificities of the Ce^{3+} $4f^1$ multiplet structure in this particular crystallographic setting, we carried out detailed quantum chemical embedded-cluster calculations. For this purpose, not only a CeO$_6$ octahedron was considered at the quantum mechanical level but also the eight Ce and ten Na nearest neighbors [see Fig. 1(b)]. The crystalline environment of this 25-site unit was modeled as a large array of point charges that reproduces the crystalline Madelung field within the cluster volume. To generate this collection of point charges we employed the EWALD package [16,17]. In a first set of computations, a fully ionic picture with formal valence states was assumed: Ce^{3+}, O^{2-}, and Na$^+$.

The actual quantum chemical calculations were performed using the MOLPRO suite of programs [18]. The numerical investigation was initiated as a complete active space self-consistent field (CASSCF) computation [19,20] with all seven $4f$ orbitals of the central Ce site incorporated in the active orbital space. The seven crystal-field states associated with the $4f^1$ manifold were obtained from a state-averaged [20]
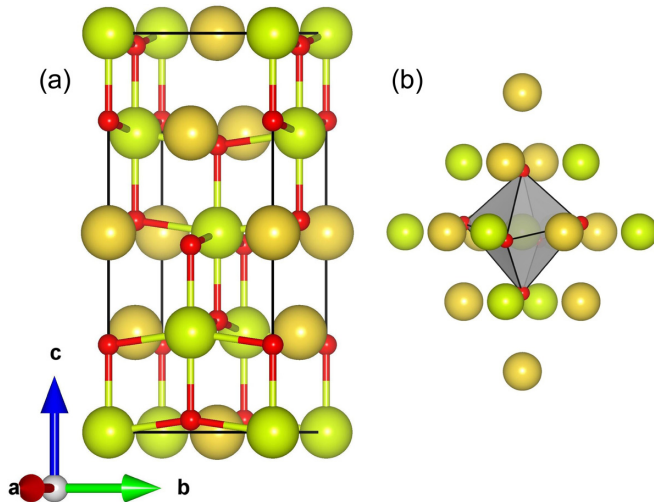
FIG. 1. (a) Unit cell of NaCeO$_2$, plotted using the VESTA visualization program [28]. Green, yellow, and red spheres indicate Ce, Na, and O species, respectively. (b) The 25-site cluster considered in the quantum chemical calculations. The crystalline environment (not depicted) was modeled as a large array of point charges in the computations.

TABLE I. Ce^{3+} $4f^1$ multiplet structure in NaCeO$_2$, with relative energies in meV. Notations as in D_{2d} symmetry are used for the crystal-field (SOC not included) and spin-orbit states (+SOC).

	CASSCF	MRSDCI	MRSDCI+SOC	INS	
$^2A_1$	0	0	0	0 ± 5	Γ_6
^2E	88	92	121	117.8 ± 1.8	Γ_7
	88	92	126	124.8 ± 1.7	Γ_7
$^2A_2$	110	110	249		Γ_6
^2E	234	238	369		Γ_6
	234	238	370		Γ_7
$^2B_2$	253	252	437		Γ_7

variational optimization. Ce $4f$ and O $2p$ electrons on the central CeO$_6$ octahedron of the 25-site cluster were subsequently considered in a multireference configuration interaction (MRCI) with single and double excitations (MRSDCI) [20,21]. Finally, spin-orbit calculations were carried out in terms of both CASSCF and MRSDCI states [22]. We used energy-consistent quasirelativistic pseudopotentials [23] and Gaussian-type valence basis sets of quadruple-ζ quality [24] for the central Ce ion, whereas for O ligands of the central CeO$_6$ octahedron we employed all-electron correlation-consistent polarized basis sets of triple-ζ quality [25]. We adopted large-core pseudopotentials including the $4f$ subshell in the core for the eight Ce nearest neighbors [26]. Large-core pseudopotentials were also considered for the ten adjacent Na cations [27].

III. Ce $4f^1$ MUTLIPLET STRUCTURE

The Ce $4f^1$ valence configuration is associated with fascinating properties, ranging from low-dimensional frustrated magnetism and possibly a spin-liquid ground state in KCeSe$_2$ [29] to Kondo physics in various intermetallic compounds [30] and multipolar states in Ce hexaboride [31,32] and Ce oxide pyrochlores [14]. CASSCF and MRSDCI results for the Ce $4f^1$ electronic structure in NaCeO$_2$, both without and with SOC, are presented in Table I. We here employed crystallographic data as reported in Ref. [9]. NaCeO$_2$ displays an $I4_1/amd$ tetragonal lattice [33] (see Fig. 1); the Wyckoff positions of Ce, Na, and O are $4a(0, 0, 0)$, $4b(0, 0, 1/2)$, and $8e(0, 0, 0.21921)$, respectively, while the experimentally determined unit-cell parameters are $a = b = 4.77860$ and $c = 11.04277$ Å [9]. A CeO$_6$ octahedron features two distinct types of Ce-O links. The Ce-O bond lengths, 2.41 and 2.42 Å, are not very different; what plays a more important role in splitting the set of six ligands into two symmetry inequivalent

groups is the farther-neighbor linkage (see Fig. 1). There are also three different O-Ce-O bond angles, of 81.9°, 91.1°, and 98.1°. As the Ce-site point group symmetry is D_{2d}, the f levels are split into three nondegenerate a_1, a_2, and b_2 and two sets of doubly degenerate e crystal-field sublevels.

As far as the crystal-field levels in NaCeO$_2$ are concerned, very large splittings of up to 250 meV are computed (first columns in Table I, results without including SOC), a few times larger than the strength of the spin-orbit coupling constant [7,34]. This is then reflected in the splittings among the spin-orbit Kramers doublets (last columns in Table I, SOC included). Experimental estimates for the relative energies of the lowest two excited states are available from inelastic neutron scattering (INS) measurements [9]. Very good agreement is found between peak positions in the INS spectra and MRSDCI+SOC results for those two low-lying on-site excited states: 118 vs 121 and 125 vs 126 meV, respectively. The *ab initio* quantum chemical data also show that the two lowest excited states lie at about the same distance with respect to the ground state and to the next excited Kramers doublet. All these electronic-structure peculiarities indicate that in NaCeO$_2$ the $J = 5/2$ and $J = 7/2$ nomenclature is not appropriate.

Splittings as large as here were earlier found in $4f^1$ delafossites [7,8], honeycombs [10], and garnets [6]. Intriguingly, one extra excitation is experimentally observed in delafossites [8,12], presumably related to vibronic effects [35]. This provides strong motivation for more systematic *ab initio* quantum chemical investigations in $4f^1$ compounds, delafossites but also other variaties such as the NaCeO$_2$ system addressed here. With anomalies in the measured spectra (e.g., extra peaks as in delafossites [8,12] and pyrochlores [13,14]), a clear assignment of the excitations is problematic at the model-Hamiltonian level.

Not surprisingly, the MRSDCI treatment brings only minor corrections to the CASSCF excitation energies, as seen by comparing data in the first two columns of Table I; having only one $4f$ electron for the leading ground-state configuration, there are only weak on-site $4f$-semicore and intersite Ce $4f$-O $2p$ correlations showing up post-CASSCF. But substantial MRSDCI corrections were found in previous studies for larger filling of the $4f$ shell, in, e.g., $4f^{13}$ compounds [36].

Knowing that valence-semicore and ligand-metal charge-transfer-type correlation effects are not significant, the very good agreement between computational and experimental re-

TABLE II. Ground-state g factors in $NaCeO_2$, by CASSCF+SOC, MRSDCI+SOC, and INS [9] (on the basis of model-Hamiltonian fits of INS peak positions).

	g_{ab}	g_c
CASSCF+SOC	1.12	0.71
MRSDCI+SOC	1.11	0.66
INS	1.41	1.00

sults convincingly validates the material model employed here: a "central" quantum mechanical cluster, a buffer region consisting of large-core effective potentials and less sophisticated valence basis functions, plus point-charge embedding. As concerns the latter, we checked how the f-f excitation energies depend on the precise values chosen for the ionic charges of the extended lattice, i.e., reduced the formal $+3$ (Ce) and -2 (O) to $+2.6$ (Ce) and -1.8 (O) [37]. The f-f excitation energies computed this way are essentially the same as in Table I [38], which shows that although less elaborated than, e.g., embeddings constructed on the basis of prior Hartree-Fock [39] or density-functional [40,41] periodic calculations, a point-charge representation of the extended crystalline surroundings is effective for ionic materials. A more sensitive aspect is how cation species in the immediate vicinity of the central quantum unit are modeled: Using for the nearby cations [see Fig. 1(b)] just bare positive charges may lead to spurious orbital polarization at the boundaries of the quantum mechanical region [42–45].

Based on the spin-orbit MRSDCI and CASSCF wave functions, we also calculated Ce-ion g factors, using the Gerloch-McMeeking formula [46] and following the pro-

cedure outlined in Ref. [47]; results are presented in Table II, along with experimentally measured g factors. It is seen that the g factors are fairly anisotropic. The magnitude of the g factors is somewhat on the lower side in the calculations as compared to the experimental estimates.

IV. CONCLUSIONS

In sum, the accuracy of an embedded-cluster material model relying on point-charge embedding and a small buffer region between the point-charge array and the quantum mechanically modeled cluster is verified for the case of a $4f^1$ oxide, $NaCeO_2$. The system is well suited to this purpose since accurate experimental data are available for the on-site f-f excitation energies and dynamical correlation effects [20] are modest for the $4f^1$ configuration. The latter feature, in particular, eliminates one possible source of errors in the electronic-structure calculations. Very good agreement with experimental results is found in the quantum chemical computations, as also seen in the case of d-electron systems with one particle per site [45]. This validates the type of embedding scheme employed here. Our analysis also indicates large $4f$-shell crystal-field splittings of up to 250 meV, which renders the J-multiplet nomenclature inappropriate [48] and confirms $NaCeO_2$ [9] as a $4f$ magnet in the intermediate coupling regime with equally strong $4f$-shell spin-orbit and crystal-field interactions.

[1] A. Kitaev, Ann. Phys. **321**, 2 (2006).

[2] G. Jackeli and G. Khaliullin, Phys. Rev. Lett. **102**, 017205 (2009).

[3] M. Moretti Sala, S. Boseggia, D. F. McMorrow, and G. Monaco, Phys. Rev. Lett. **112**, 026403 (2014).

[4] N. A. Bogdanov, V. M. Katukuri, H. Stoll, J. van den Brink, and L. Hozoi, Phys. Rev. B **85**, 235147 (2012).

[5] G. Bastien, G. Garbarino, R. Yadav, F. J. Martinez-Casado, R. Beltrán Rodríguez, Q. Stahl, M. Kusch, S. P. Limandri, R. Ray, P. Lampen-Kelley, D. G. Mandrus, S. E. Nagler, M. Roslova, A. Isaeva, T. Doert, L. Hozoi, A. U. B. Wolter, B. Büchner, J. Geck, and J. van den Brink, Phys. Rev. B **97**, 241108(R) (2018).

[6] L. Seijo and Z. Barandiaran, Phys. Chem. Chem. Phys. **16**, 3830 (2014).

[7] M. S. Eldeeb, T. Petersen, L. Hozoi, V. Yushankhai, and U. K. Rössler, Phys. Rev. Materials **4**, 124001 (2020).

[8] M. M. Bordelon, X. Wang, D. M. Pajerowski, A. Banerjee, M. Sherwin, C. M. Brown, M. S. Eldeeb, T. Petersen, L. Hozoi, U. K. Rössler, M. Mourigal, and S. D. Wilson, Phys. Rev. B **104**, 094421 (2021).

[9] M. M. Bordelon, J. D. Bocarsly, L. Posthuma, A. Banerjee, Q. Zhang, and S. D. Wilson, Phys. Rev. B **103**, 024430 (2021).

[10] M. J. Daum, A. Ramanathan, A. I. Kolesnikov, S. Calder, M. Mourigal, and H. S. La Pierre, Phys. Rev. B **103**, L121109 (2021).

[11] See, e.g., the discussion in Ref. [6].

[12] G. Bastien, B. Rubrecht, E. Haeussler, P. Schlender, Z. Zangeneh, S. Avdoshenko, R. Sarkar, A. Alfonsov, S. Luther, Y. A. Onykiienko et al., SciPost Phys. **9**, 041 (2020).

[13] J. Gaudet, E. M. Smith, J. Dudemaine, J. Beare, C. R. C. Buhariwalla, N. P. Butch, M. B. Stone, A. I. Kolesnikov, G. Xu, D. R. Yahne, K. A. Ross, C. A. Marjerrison, J. D. Garrett, G. M. Luke, A. D. Bianchi, and B. D. Gaulin, Phys. Rev. Lett. **122**, 187201 (2019).

[14] R. Sibille, N. Gauthier, E. Lhotel, V. Pore, V. Pomjakushin, R. A. Ewings, T. G. Perring, J. Ollivier, A. Wildes, C. Ritter, T. C. Hansen, D. A. Keen, G. J. Nilsen, L. Keller, S. Petit, and T. Fennell, Nat. Phys. **16**, 546 (2020).

[15] Y. Y. Pai, C. E. Marvinney, L. Liang, J. Xing, A. Scheie, A. A. Puretzky, G. B. Halasz, X. Li, R. Juneja, A. S. Sefat, D. Parker,

L. Lindsay, and B. J. Lawrie, J. Mater. Chem. C **10**, 4148 (2022).

[16] M. Klintenberg, S. Derenzo, and M. Weber, Comput. Phys. Commun. **131**, 120 (2000).

[17] S. E. Derenzo, M. K. Klintenberg, and M. J. Weber, J. Chem. Phys. **112**, 2074 (2000).

[18] H.-J. Werner, P. J. Knowles, G. Knizia, F. R. Manby, and M. Schütz, WIREs Comput. Mol. Sci. **2**, 242 (2012).

[19] D. A. Kreplin, P. J. Knowles, and H.-J. Werner, J. Chem. Phys. **152**, 074102 (2020).

[20] T. Helgaker, P. Jørgensen, and J. Olsen, *Molecular Electronic Structure Theory* (Wiley, Chichester, UK, 2000).

[21] P. J. Knowles and H.-J. Werner, Theor. Chim. Acta **84**, 95 (1992).

[22] A. Berning, M. Schweizer, H.-J. Werner, P. J. Knowles, and P. Palmieri, Mol. Phys. **98**, 1823 (2000).

[23] M. Dolg, H. Stoll, and H. Preuss, J. Chem. Phys. **90**, 1730 (1989).

[24] X. Cao and M. Dolg, J. Mol. Struc.: THEOCHEM **581**, 139 (2002).

[25] T. H. Dunning, J. Chem. Phys. **90**, 1007 (1989).

[26] M. Dolg, H. Stoll, A. Savin, and H. Preuss, Theor. Chim. Acta **75**, 173 (1989).

[27] P. Fuentealba, H. Preuss, H. Stoll, and L. Von Szentpály, Chem. Phys. Lett. **89**, 418 (1982).

[28] K. Momma and F. Izumi, J. Appl. Crystallogr. **44**, 1272 (2011).

[29] L. D. Sanjeewa, J. Xing, K. M. Taddei, and A. S. Sefat, J. Solid State Chem. **308**, 122917 (2022).

[30] P. Fulde, *Correlated Electrons in Quantum Matter* (World Scientific, Singapore, 2012).

[31] A. S. Cameron, G. Friemel, and D. S. Inosov, Rep. Prog. Phys. **79**, 066502 (2016).

[32] P. Thalmeier, A. Akbari, and R. Shiina, *Multipolar Order and Excitations in Rare-Earth Boride Kondo Systems* (Taylor & Francis, New York, 2021).

[33] M. M. Bordelon, C. Liu, L. Posthuma, E. Kenney, M. J. Graf, N. P. Butch, A. Banerjee, S. Calder, L. Balents, and S. D. Wilson, Phys. Rev. B **103**, 014420 (2021).

[34] D. Aravena, M. Atanasov, and F. Neese, Inorg. Chem. **55**, 4457 (2016).

[35] H. Gerlinger and G. Schaack, Phys. Rev. B **33**, 7438 (1986).

[36] Z. Zangeneh, S. Avdoshenko, J. van den Brink, and L. Hozoi, Phys. Rev. B **100**, 174436 (2019).

[37] In other words, the Madelung potential in the cluster region (25 sites) corresponds in this set of calculations to a periodic structure with $+1$, $+2.6$, and -1.8 point charges at the Na, Ce, and O lattice sites. Overall charge neutrality is preserved by a subsequent slight readjustment of O charges in the immediate neighborhood of the 25-site central fragment.

[38] Variations within 1 meV are found.

[39] L. Hozoi, U. Birkenheuer, H. Stoll, and P. Fulde, New J. Phys. **11**, 023023 (2009).

[40] A. S. P. Gomes, C. R. Jacob, and L. Visscher, Phys. Chem. Chem. Phys. **10**, 5353 (2008).

[41] M. Zbiri, M. Atanasov, C. Daul, J. M. Garcia-Lastra, and T. A. Wesolowski, Chem. Phys. Lett. **397**, 441 (2004).

[42] J. L. Pascual, L. Seijo, and Z. Barandiarán, J. Chem. Phys. **98**, 9715 (1993).

[43] C. de Graaf, C. Sousa, and R. Broer, J. Mol. Struc.: THEOCHEM **458**, 53 (1998).

[44] L. Hozoi, L. Siurakshina, P. Fulde, and J. van den Brink, Sci. Rep. **1**, 65 (2011).

[45] N. A. Bogdanov, J. van den Brink, and L. Hozoi, Phys. Rev. B **84**, 235146 (2011).

[46] H. Bolvin, ChemPhysChem **7**, 1575 (2006).

[47] N. A. Bogdanov, V. M. Katukuri, J. Romhányi, V. Yushankhai, V. Kataev, B. Büchner, J. van den Brink, and L. Hozoi, Nat. Commun. **6**, 7306 (2015).

[48] N. Magnani, P. Santini, G. Amoretti, and R. Caciuffo, Phys. Rev. B **71**, 054405 (2005).